Plant Physiology®

Plant Physiology, 2024, **196**, 397–408
https://doi.org/10.1093/plphys/kiae319
Advance access publication 7 June 2024
Research Article

Absence of alka(e)nes triggers profound remodeling of glycerolipid and carotenoid composition in cyanobacteria membrane

Rui Miao,[1,2,*] Bertrand Légeret,[1] Stéphan Cuine,[1] Adrien Burlacot,[1,3] Peter Lindblad,[2] Yonghua Li-Beisson,[1] Fred Beisson,[1] and Gilles Peltier[1,*]

[1]Institut de Biosciences et Biotechnologies, Aix Marseille Univ, CEA, CNRS, BIAM, Saint Paul-Lez-Durance, F-13115, France
[2]Microbial chemistry, Department of Chemistry-Ångström Laboratory, Uppsala University, Box 523, SE-751 20 Uppsala, Sweden
[3]Carnegie Institution for Science, Department of Plant Biology, 260 Panama Street, Stanford, CA 94305, USA
*Author for correspondence: rui.miao@kemi.uu.se (R.M), gilles.peltier@cea.fr (G.P)
The author responsible for distribution of materials integral to the findings presented in this article in accordance with the policy described in the Instructions for Authors (https://academic.oup.com/plphys/pages/General-Instructions) is Rui Miao.

Abstract

Alka(e)nes are produced by many living organisms and exhibit diverse physiological roles, reflecting a high functional versatility. Alka(e)nes serve as waterproof wax in plants, communicating pheromones for insects, and microbial signaling molecules in some bacteria. Although alka(e)nes have been found in cyanobacteria and algal chloroplasts, their importance for photosynthetic membranes has remained elusive. In this study, we investigated the consequences of the absence of alka(e)nes on membrane lipid composition and photosynthesis using the cyanobacterium *Synechocystis* PCC6803 as a model organism. By following the dynamics of membrane lipids and the photosynthetic performance in strains defected and altered in alka(e)ne biosynthesis, we show that drastic changes in the glycerolipid contents occur in the absence of alka(e)nes, including a decrease in the membrane carotenoid content, a decrease in some digalactosyldiacylglycerol (DGDG) species and a parallel increase in monogalactosyldiacylglycerol (MGDG) species. These changes are associated with a higher susceptibility of photosynthesis and growth to high light in alka(e)ne-deficient strains. All these phenotypes are reversed by expressing an algal photoenzyme producing alka(e)nes from fatty acids. Therefore, alkenes, despite their low abundance, are an essential component of the lipid composition of membranes. The profound remodeling of lipid composition that results from their absence suggests that they play an important role in one or more membrane properties in cyanobacteria. Moreover, the lipid compensatory mechanism observed is not sufficient to restore normal functioning of the photosynthetic membranes, particularly under high-light intensity. We conclude that alka(e)nes play a crucial role in maintaining the lipid homeostasis of thylakoid membranes, thereby contributing to the proper functioning of photosynthesis, particularly under elevated light intensities.

Introduction

Alkanes (saturated) and alkenes (unsaturated), both classes of acyclic hydrocarbons and the principal components of fossil fuels, are ubiquitous in our daily lives, serving diverse functions and applications. Remarkably, alka(e)nes are not confined to the realm of fossil fuels; numerous organisms across the biological kingdom also synthesize them, each with distinct carbon chain lengths, cellular locations, and physiological functions. For instance, insects primarily synthesize very-long-chain linear alka(e)nes (*n*-alka(e)nes) through a process that involves fatty acid elongation, reduction to aldehyde, and subsequent oxidative decarbonylation (Major and Blomquist 1978; Laurent et al. 2003; Blomquist and Ginzel 2021). These *n*-alka(e)nes serve essential roles in preventing desiccation and act as potent sensory neuron activators during defensive and reproductive behaviors (Chung and Carroll 2015; Blomquist and Ginzel 2021). Plants also synthesize *n*-alka(e)nes from fatty acids, with cuticular waxes enriched in very-long-chain alkanes providing protection against desiccation and environmental stressors like UV radiation and pathogens (Yeats and Rose 2013; Lee and Suh 2022). Among unicellular organisms, some non-photosynthetic bacteria have the ability to naturally produce alka(e)nes, primarily via the decarbonylation of fatty aldehydes or decarboxylation of fatty acids (Valderrama 2004; Herman and Zhang 2016). As photosynthetic microorganisms, microalgae also harbor a distinctive pathway for alka(e)ne synthesis (Sorigué et al. 2016). The discovery of FAP in green microalgae (Sorigué et al. 2017) has enriched our repertoire of alka(e)ne-forming enzymes because of the unique photocatalytic process of FAP, which converts free fatty acids (FFA) to alka(e)nes using light in the range 350 to 530 nm (Sorigué et al. 2021; Samire et al. 2023). FAP belongs to an algal-specific clade of glucose methanol choline (GMC) oxidoreductase family and phylogenetic analysis showed that this photoenzyme is conserved in photosynthesis-retained algal lineages (Moulin et al. 2021). Cyanobacteria are known to harbor two mutually exclusive alka(e)ne synthesis pathways: the acyl-ACP reductase (Aar) and aldehyde deformylating oxygenase (Ado) pathway (Schirmer et al. 2010) and the olefin synthase (Ols) pathway (Mendez-Perez

Received April 5, 2024. Accepted April 29, 2024.
© The Author(s) 2024. Published by Oxford University Press on behalf of American Society of Plant Biologists.
This is an Open Access article distributed under the terms of the Creative Commons Attribution-NonCommercial-NoDerivs licence (https://creativecommons.org/licenses/by-nc-nd/4.0/), which permits non-commercial reproduction and distribution of the work, in any medium, provided the original work is not altered or transformed in any way, and that the work is properly cited. For commercial re-use, please contact reprints@oup.com for reprints and translation rights for reprints. All other permissions can be obtained through our RightsLink service via the Permissions link on the article page on our site—for further information please contact journals.permissions@oup.com.

Downloaded from https://academic.oup.com/plphys/article/196/1/397/7689884 by The Uppsala Programme for Holocaust and Genocide studies user on 05 November 2024

Begemann and Pfleger 2011). In a survey of 73 cyanobacterial strains spanning a broad phylogenetic range, it was found that the vast majority possessed the Aar–Ado pathway and only 12 strains, two-thirds of which were from a single clade, possessed the Ols pathway (Coates et al. 2014). It is interesting to note that while the alkanes and alkenes synthesized by cyanobacteria and microalgae represent only a few percent of most of their total fatty acids, on a global scale this synthesis is not anecdotal, as an oceanic cycle of long-chain alkanes produced by marine cyanobacteria (and also probably microalgae) has been identified and characterized (Lea-Smith et al. 2015; Love et al. 2021).

The diverse alka(e)ne biosynthesis pathways in nature highlight the intricate evolutionary adaptations of organisms to their ecological niches and the multifaceted roles of alka(e)nes in various biological contexts. Notably, orthologous genes to *aar* and *ado* have been identified exclusively in cyanobacteria so far, implying a potential connection to a photoautotrophic lifestyle (Klähn et al. 2014). Photosynthesis, a delicate and complex process, relies on the complex structure and fluidity of cellular membranes, particularly the thylakoid membrane where light-dependent reactions occur. In the model microalga *Chlamydomonas reinhardtii*, FAP and its major product 7-heptadecene were found associated with the thylakoid membranes in the chloroplast, and the study of a FAP knockout mutant suggested a role for this alkene in photosynthesis under cold and varying light conditions but the exact molecular mechanism remains unknown (Moulin et al. 2021). The physiological function of the native intracellular alka(e)nes has been recently investigated in cyanobacteria. The study of strains deficient in the *aar/ado* pathway revealed various deficiencies, including impairment in cell division, reduced CO_2 uptake and oxygen evolution, and increased sensitivity to low temperature or salt stress (Berla et al. 2015; Lea-Smith et al. 2016; Yamamori et al. 2018; Vuorio et al. 2021). It has also been shown that as the temperature shifts from 38 °C down to 15 °C, the proportion of saturated heptadecane to unsaturated heptadecene decreases, yet the overall hydrocarbon content remains relatively unchanged (Vuorio et al. 2021). Molecular dynamics simulation suggests that alka(e)nes localize in the middle part of the lipid bilayer and may play a role in membranes by promoting flexibility and facilitating curvature (Lea-Smith et al. 2016). However, there is a gap in experimental research exploring the downstream effects of this altered curvature on thylakoid membrane function and organization.

In this study, we aimed to bridge this gap by examining how a deficiency in alka(e)ne influences lipidome dynamics and photosynthetic activity in response to varying light conditions. We show that the absence of alkanes/alkenes causes perturbations to membrane lipid composition thus promoting the instability of PSI trimers and the high-light sensitivity of photosynthesis. We conclude that hydrocarbons contribute to membrane lipid homeostasis, which is critical for the photosynthetic apparatus to withstand high-light intensity.

Results

Absence of alka(e)nes affect cell ultrastructure

In *Synechocystis*, as in many other cyanobacterial strains, the acyl-ACP reductase encoding gene *aar* and the deformylating oxygenase encoding gene *ado* are transcribed in two neighboring operons (Coates et al. 2014; Klähn et al. 2014). Two transcription start sites (TSS) have been identified at the 5′-end of the *ado* gene, which may imply the potential transcription of multiple isoforms under specific conditions (Klähn et al. 2014). Considering the regulatory implications of such complex transcriptional organization, we generated three alka(e)ne-deficient *Synechocystis* strains, ΔAdo, ΔAar, and ΔAdoAar. The deformylating oxygenase Ado uses an external reducing system capable of supplying four electrons for each catalytic cycle, so alka(e)ne synthesis has been considered as an electron sink to dissipate excess energy in specific conditions (Li et al. 2011; Klähn et al. 2014). Therefore, to attribute observed phenotypes to alkanes by avoiding the potential effects of electron consumption and metabolic intermediates, we used the photoenzyme FAP from *Chlorella variabilis* (Sorigué et al. 2017) to functionally complement strains deficient in alka(e)nes. Unlike the Aar–Ado pathway, which utilizes acyl-ACPs as substrates and produces fatty aldehydes as intermediates, the FAP enzyme catalyzes the decarboxylation of free fatty acid in a single step, requiring light in the range of 350 to 530 nm.

FAP and a chloramphenicol resistance gene were integrated into the genome of each alka(e)ne-deficient strain at the *slr1993* locus, resulting in strains ΔAdo-FAP, ΔAar-FAP, and ΔAdoAar-FAP. In *Synechocystis*, the gene *slr1993* is responsible for coding the acetyl-CoA acetyltransferase PhaA, which plays a role in the polyhydroxybutyrate (PHB) synthesis pathway. Extensive comparisons between wild-type *Synechocystis* and strains lacking the PHB synthesis pathway have been conducted across a spectrum of more than ten different cultivation conditions, including various stress environments (Koch Berendzen and Forchhammer 2020). Under none of the tested conditions, PHB-deficient strains showed a fitness difference as compared to the WT. To ensure all the phenotype changes in strains expressing FAP are not contributed by the deletion of *slr1993*, we generated corresponding control strains denoted as ΔAdo-FAP control, ΔAar-FAP control, and ΔAdoAar-FAP control by integrating a chloramphenicol resistance gene at *slr1993* locus. As previously reported (Schirmer et al. 2010; Coates et al. 2014), the major alka(e)ne produced by *Synechocystis* was found to be *n*-heptadecane (C17 *n*-alkane), but minor amounts of *n*-pentadecane (C15 *n*-alkane) and two heptadecene isomers (C17 mono-alkene) were also detected (Fig. 1A). As anticipated, no alka(e)nes were detectable in strains ΔAdo, ΔAar, and ΔAdoAar. Complemented strains expressing FAP produced the same type of alka(e)nes as the WT strain, while at lower amounts particularly for the more abundant species heptadecane (Fig. 1A).

In line with a previous study (Lea-Smith et al. 2016), we observed that the cell size of the alka(e)ne-deficient strains exhibited a significant increase, with dimensions nearly doubling that of both the WT strain and the complemented strains (Fig. 1B). Because strains ΔAdo, ΔAar, and ΔAdoAar always showed similar phenotypes (Supplementary Fig. S1), further experiments were performed on one of them, ΔAdo, and its corresponding controls. To further gain information on subcellular changes, we examined the cells under transmission electron microscopy (TEM) which revealed a profound impact on the organization of thylakoid membranes in the absence of alka(e)nes (Fig. 1C and Supplementary Fig. S2). While the WT and complemented strains consistently exhibited around four to five thylakoid layers per cell, the alka(e)ne-deficient contained around seven to eight apparent layers of thylakoid membranes per cell (Fig. 1C and Supplementary Fig. S3). This transformation in thylakoid structure suggests a key role for alka(e)nes in maintaining membrane architecture, with potential repercussions on photosynthetic capacity.

Alka(e)nes are critical for cell growth and photosynthesis under high light

We then aimed to determine whether alka(e)ne deficiency affects photoautotrophic growth by performing growth tests on solid media under varying light intensities. For each strain, experiments

Downloaded from https://academic.oup.com/plphys/article/196/1/397/7689884 by The Uppsala Programme for Holocaust and Genocide studies user on 05 November 2024

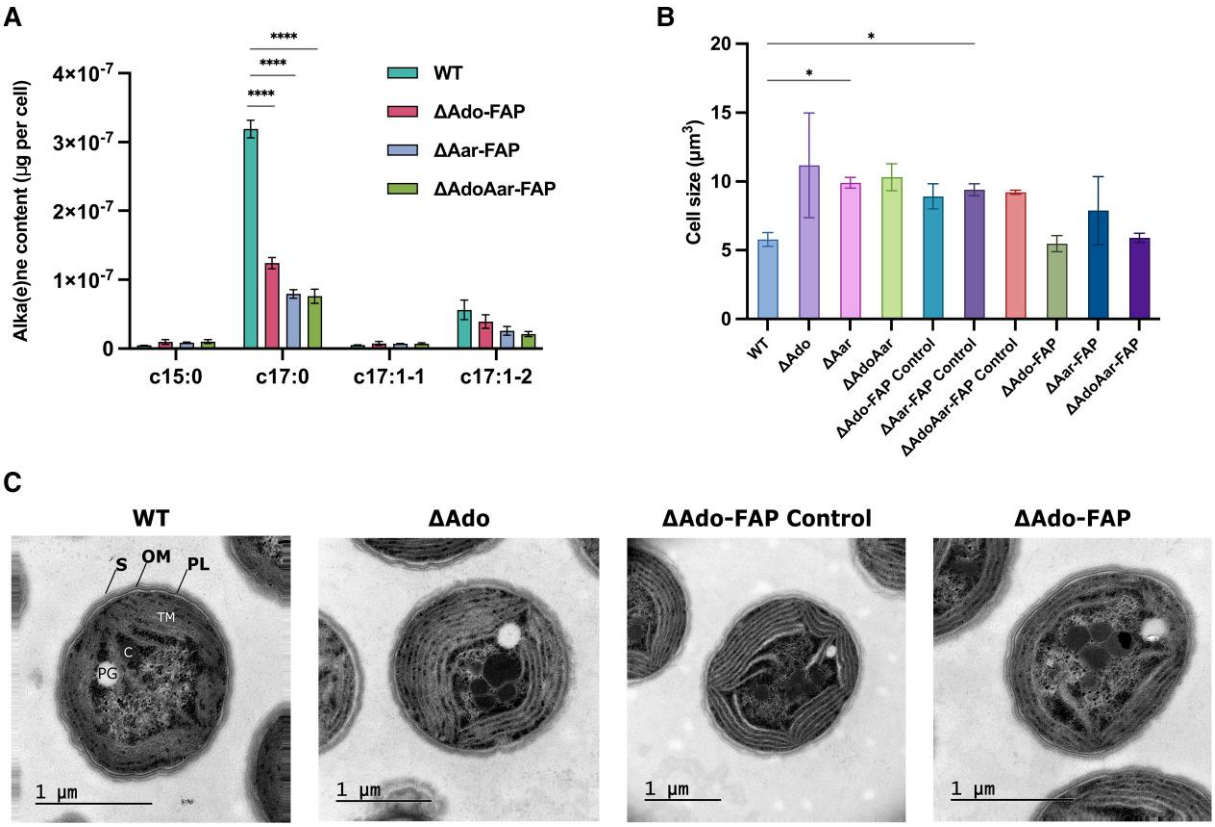

Figure 1. Alka(e)nes production, cell size, and cell morphology in *synechocystis* PCC6803 strains cultivated under 30 μmol photon m^{-2} s^{-1}. **A)** Alka(e)nes production in wild-type and all complemented strains. Alka(e)nes were quantified from mid-log phase (OD_{730} = 0.6) cultures using transmethylation of cells and GC-MS analysis. Alka(e)ne production was normalized to cell number. Results represent the mean of three biological replicates; error bars represent standard deviation. Two-way ANOVA was used to determine statistical significance (*P* value < 0.05). **B)** Cell size comparison among all strains. All cells were grown to mid-log phase (OD_{730} = 0.6), and cell volume was measured using a Coulter counter. Results represent the mean of 3 biological replicates; error bars represent standard deviation. One-way ANOVA was used to determine significance (*P* value < 0.05). **C)** Transmission electron microscopy images. All cells were grown to OD_{730} = 0.3 and then for room temperature fixation. TM: thylakoid membrane; C: carboxysome; PG: polyphosphate granule; PL: peptidoglycan layer; OM: outer membrane; S: S-layer.

were initiated with three different initial cell concentrations. While no growth difference was observed under low light (20 μmol photons m^{-2} s^{-1}) between the different strains, a significant growth defect was observed in all alka(e)ne-deficient strains under medium light (50 μmol photons m^{-2} s^{-1}), and a complete growth arrest under high light (200 μmol photons m^{-2} s^{-1}) (Fig. 2A). Remarkably, this growth phenotype was fully restored in the complemented line despite a lower accumulation of alkanes as compared to the WT strain (Fig. 1A).

We then investigated the effects of alka(e)ne deficiency on photosynthesis. For this purpose, we performed chlorophyll fluorescence measurements to determine the max PSII efficiency (Fv/Fm), the operating PSII quantum yield under actinic light (ΦPSII), and energy dissipation by non-photochemical quenching (NPQ). Since the determination of PSII yields from chlorophyll fluorescence is not straightforward in cyanobacteria due to the presence of phycobilisomes (Schuurmans et al. 2015), we simultaneously measured O_2 exchange by using membrane inlet mass spectrometry (MIMS) in the presence of ^{18}O-labeled O_2, which allows determining gross O_2 production rates by PSII and O_2 consumption rates in the light (Burlacot et al. 2020). These measurements were performed in response to different illumination regimes, with cells grown under either low light (10 μmol photons m^{-2} s^{-1}) or relatively high light (70 μmol photons m^{-2} s^{-1}). When the different *Synechocystis* strains were grown under low light, no significant changes in Fv/Fm, ΦPSII, NPQ, and O_2 exchange were observed among all the strains (Fig. 2 B and C and Supplementary Fig. S4). When cultivated under higher light intensity, the alka(e)ne-deficient strains exhibited significantly lower Fv/Fm and ΦPSII values, along with increased NPQ, compared to the WT under actinic illumination. This effect was reversed in the functionally complemented strain expressing FAP (Fig. 2 B and C). Note here that due to the background fluorescence of phycobilisomes, ΦPSII and ΦNPQ values determined here should be only considered as relative values. In line with chlorophyll fluorescence measurements, both gross and net O_2 production rates were decreased in the alka(e)ne-deficient strains grown under high-light intensity (Fig. 2C), while the O_2 uptake rate was mostly unaffected (Supplementary Fig. S4). We then analyzed the distribution of chlorophyll protein complexes by performing a native PAGE on the thylakoid membrane prepared from the cells cultivated under high light. Whereas PSII-complexes were mostly unaffected, we observed a dramatic reduction in the PSI trimer content in alka(e)nes-deficient strains (Fig. 2D and Supplementary Fig. S5), thus indicating that PSI trimerization and/or stabilization might depend on the presence of alka(e)nes in the thylakoid membrane. We conclude from these results that the absence of alka(e)nes strongly affects the photosynthetic machinery and its functioning under high light.

Downloaded from https://academic.oup.com/plphys/article/196/1/397/7689884 by The Uppsala Programme for Holocaust and Genocide studies user on 05 November 2024

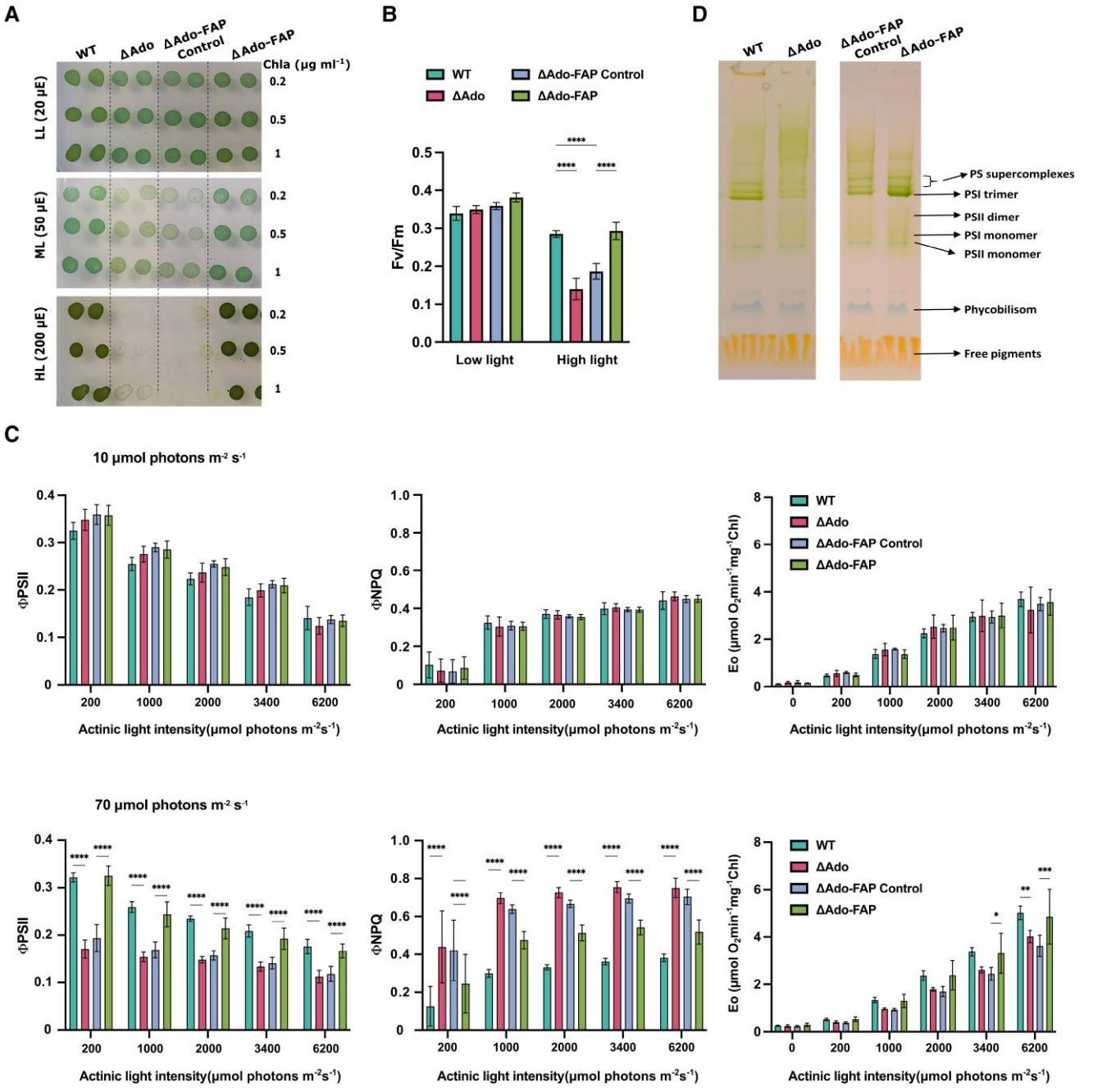

Figure 2. Alka(e)nes effects on cell growth test and photosynthetic capacity. **A)** Growth test on BG-11 agar plate under different light intensities. Biological duplicate and three different chlorophyll concentrations were used for each strain. (1) Wild-type, (2) ΔAdo, (3) ΔAdo-FAP Control, and (4) ΔAdo-FAP. **B)** The quantum yield (Fv/Fm) for dark-adapted cells was measured after 10 min of darkness adaptation. These cells had previously been cultivated under either low-light or high-light conditions. **C)** Simultaneous measurements of operating PSII quantum yield (ΦPSII), non-photochemical quenching yield (ΦNPQ), and Membrane-inlet-mass-spectrometry (MIMS) measured gross O_2 production rates (Eo) on cultures grown under both low and high light conditions. All the measurements were done under increased blue actinic light. Results in B and C represent the mean of 3 biological replicates; error bars represent standard deviation, and significance (P value < 0.05) was determined using two-way ANOVA. **D)** Clear-native PAGE (CN-PAGE) on thylakoid membrane extracts from cells grown under 70 μmol photons m^{-2} s^{-1}. Extraction was done on mid-log phase (OD730 = 0.6) cells. Thylakoid membranes were quantified according to the chlorophyll content. Samples containing the same amount of chlorophyll were loaded on the gel. (1) Wild-type, (2) ΔAdo, (3) ΔAdo-FAP Control, and (4) ΔAdo-FAP.

The cyanobacterial lipidome is drastically remodeled in the absence of alka(e)nes

Given the close link between alka(e)ne and fatty acid biosynthetic pathways (Supplementary Fig. S6), and the altered ultrastructures of photosynthetic membranes observed in alka(e)ne-deficient strains, we sought to analyze in depth the effect of alka(e)ne deficiency on the lipidome. We first analyzed changes in the fatty acid content of the various strains cultivated under either low light (10 μmol photons m^{-2} s^{-1}) or high light (70 μmol photons m^{-2} s^{-1}). Under low light, alka(e)ne-deficient strains exhibited higher contents of C16:0, C16:1, and C18:1 fatty acids as compared to WT and complemented strains (Fig. 3A). In contrast, under high light, alka(e)ne-deficient strains showed lower contents of C16:0 and C16:1 than the WT and complemented strains. However,

Downloaded from https://academic.oup.com/plphys/article/196/1/397/7689884 by The Uppsala Programme for Holocaust and Genocide studies user on 05 November 2024

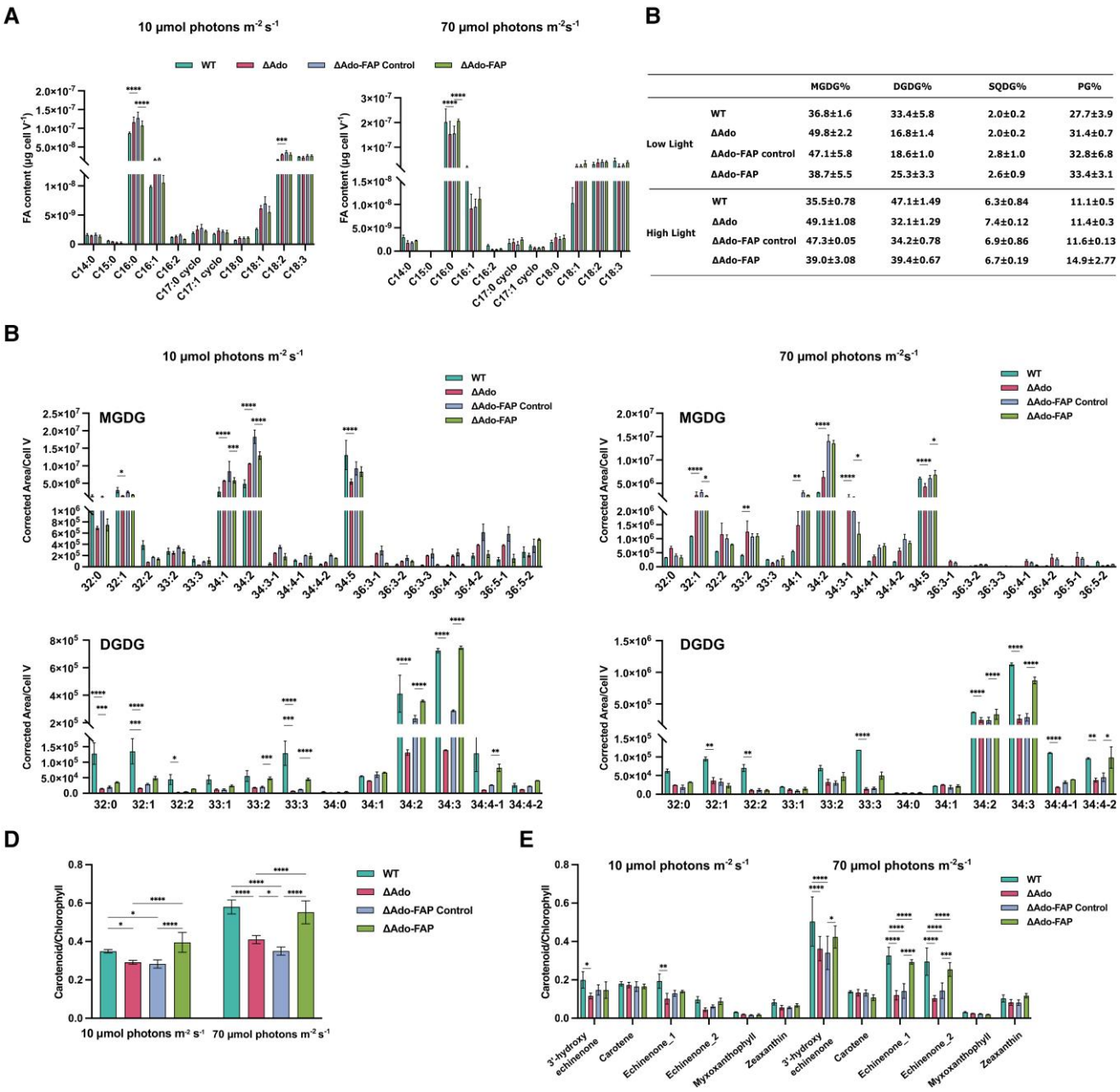

B

		MGDG%	DGDG%	SQDG%	PG%
Low Light	WT	36.8±1.6	33.4±5.8	2.0±0.2	27.7±3.9
	ΔAdo	49.8±2.2	16.8±1.4	2.0±0.2	31.4±0.7
	ΔAdo-FAP control	47.1±5.8	18.6±1.0	2.8±1.0	32.8±6.8
	ΔAdo-FAP	38.7±5.5	25.3±3.3	2.6±0.9	33.4±3.1
High Light	WT	35.5±0.78	47.1±1.49	6.3±0.84	11.1±0.5
	ΔAdo	49.1±1.08	32.1±1.29	7.4±0.12	11.4±0.3
	ΔAdo-FAP control	47.3±0.05	34.2±0.78	6.9±0.86	11.6±0.13
	ΔAdo-FAP	39.0±3.08	39.4±0.67	6.7±0.19	14.9±2.77

Figure 3. Fatty acid content, composition in major membrane glycerolipids, and carotenoid to chlorophyll ratio under low and high light intensities. **A)** Fatty acid content in *Synechocystis* strains. The contents of different fatty acid species were quantified by cell transmethylation and GC-MS and normalized to cell volume representing biomass. **B)** The proportion of MGDG and DGDG in total lipid content, and MGDG to DGDG ratio in *Synechocystis* strains. Absolute quantification of each lipid class was performed using HPTLC and densitometry. Results represent the mean of three biological replicates; ± represents standard deviation. **C)** Lipidomics analysis on DGDG and MGDG species in different strains. Results represent the mean of 3 biological replicates; error bars represent standard deviation. **D)** Spectrophotometer measured carotenoids to chlorophyll content ratio in low-light and high light cultivated strains. Pigment extraction was done using 90% pre-cold methanol. **E)** Different Carotenoid species to chlorophyll ratio measured by LC-MS. Left panel shows pigment ratio under low light and right panel shows pigment ratio under high light. Carotenoids and chlorophyll were extracted from the mid-log phase ($OD_{730} = 0.6$) culture using 90% pre-cold methanol, and then, the extracts were measured on LC-MS. All results in A, C, D, and E represent the mean of 3 biological replicates; error bars represent standard deviation, and significance (P value < 0.05) was determined using ANOVA.

the proportion of saturated-, unsaturated-, and cyclo-fatty acids remained unchanged among the strains under both low and high light (Supplementary Fig. S7).

The composition of major membrane lipid classes was then analyzed using high-performance thin-layer chromatography (HPTLC). Alka(e)ne-deficient strains consistently exhibited higher contents of the non-bilayer-forming lipid monogalactosyldiacylglycerol (MGDG) and lower contents of the bilayer-forming lipid digalactosyldiacylglycerol (DGDG) than the WT and complemented strains, irrespective of light conditions, while sulfoquinovosyldiacylglycerol (SQDG) and phosphatidylglycerol (PG) contents remained relatively constant (Fig. 3B and Supplementary Fig. S8). To gain further insights into the dynamic changes of MGDG and DGDG lipid species, we performed a comprehensive liquid chromatography-mass spectrometry (LC-MS) lipidomic analysis of glycerolipid molecular species which

Downloaded from https://academic.oup.com/plphys/article/196/1/397/7689884 by The Uppsala Programme for Holocaust and Genocide studies user on 05 November 2024

provides a relative quantification and allows to compare the dynamics of specific lipid species across different strains or experimental conditions (Fig. 3C). This analysis showed that the content of all DGDG species analyzed decreased in alka(e)ne-deficient strains regardless of light conditions (Fig. 3C). In parallel, the amount of most MGDG species increased in the absence of alka(e)nes. Notably, the expression of FAP led to a partial recovery of several DGDG species (e.g. 32:1 and 33:3), with a nearly complete recovery observed for some of them (e.g. 34:2 and 34:3). For MGDG species, FAP expression facilitated the recovery of nearly half of these lipid species, with no observable recovery for others (e.g. 32:1 and 34:2).

The major changes observed in the lipid composition of alka(e)ne-deficient strains prompted us to analyze the potential impact on pigment composition, since carotenoids are primarily located within the thylakoid membranes, where they are integrated alongside chlorophyll molecules and other pigments in the photosynthetic complexes. Carotenoids participate in light absorption and photoprotection (Kirilovsky and Kerfeld 2012), and have been shown to respond to challenging environmental conditions, such as intense light and high temperatures (Havaux 1998; Dhami et al. 2020). In low-light conditions, the carotenoid content of alka(e)ne-deficient strains was slightly lower than the WT strain (Fig. 3D), mainly due to the decrease in 3-hydroxy echinenone and two echinenone isoforms (Fig. 3E). Under high-light conditions, the carotenoid content of the WT strain increased (Fig. 3D), due to the increase of 3-hydroxy echinenone and the two echinenone isoforms (Fig. 3E), the increase being reduced in alka(e)ne-deficient strains. Complemented strains expressing FAP showed recovery of all carotenoids (Fig. 3E) under both light conditions. We did not observe a significant change in chlorophyll content from cultures grown under the same light condition (Supplementary Fig. S9), indicating that observed changes in carotenoids do not reflect a decline in all photosynthetic pigments.

Discussion

In this study, we investigated the physiological role of alka(e)nes in relation to the photosynthetic function, using the cyanobacterium *Synechocystis* PCC6803 as a model organism. The absence of alka(e)nes provoked remarkable structural and physiological changes, including an altered pigment content, a profound remodeling of the glycerolipid composition of the thylakoid membranes, and a growth defect under high-light intensity. Specifically, when alka(e)ne-deficient strains were cultivated under high light, the photosynthetic activity was reduced, and the non-photochemical quenching increased. The lipidomics analysis revealed a decrease in DGDG and an increase in MGDG levels together with a decrease in the carotenoid content in alka(e)ne-deficient strains in both low- and high-light conditions. All of the observed phenotypes could be either partially or completely restored when the alka(e)ne-producing photoenzyme FAP was expressed in the mutant strains.

Alka(e)nes deficiency affects thylakoid membrane dynamics

A molecular dynamics simulation has suggested that the alka(e)nes located in the center of the bilayer membrane would contribute to membrane flexibility thus facilitating membrane curvature (Lea-Smith et al. 2016). Therefore, the decreased MGDG to DGDG ratio in the absence of alka(e)ne regardless of cultivation light suggests a primary compensatory effect that may stem from the lack of membrane flexibility and curvature. MGDG is one of the most abundant lipids in thylakoid membranes and has a cone-shaped molecular structure. This shape tends to promote the formation of non-bilayer (hexagonal II) phases, which are more fluid. MGDG is known to play a crucial role in maintaining the fluidity of the thylakoid membrane and is vital for the proper functioning of the photosynthetic machinery (Marsh 1996; Hoyo Guaus and Torrent-Burgués 2016). On the other hand, DGDG, with its more cylindrical shape due to the addition of another galactose group, favors bilayer formation. DGDG can contribute to membrane rigidity and stability, especially under stress conditions. For instance, under phosphate-limited conditions, DGDG can substitute for phospholipids in various membranes to ensure membrane stability (Härtel Dormann and Benning 2000; Andersson and Dörmann 2008).

The absence of alka(e)nes did not only impact the glycerolipid composition in the thylakoid membranes, and it also had an effect on the associated carotenoids. Carotenoids are tetra-terpenoid

molecules found in all photosynthetic organisms, playing a key role in enhanced light absorption and energy dissipation during photosynthesis (Pagels Vasconcelos and Guedes 2021). In our alka(e)ne-deficient strains, lower carotenoid content was observed regardless of light and CO_2 availability (Supplementary Fig. S10). This result is in line with a previous observation of a lower relative amount of carotenoids in comparison with chlorophyll and phycocyanin in Δado strain at low temperatures (Vuorio et al. 2021). As for the MGDG/DGDG ratio, the alteration of the carotenoid content could be a compensatory effect directly from the change of membrane fluidity, or result from changes in the lipid environment. It has been shown that in Arabidopsis (*Arabidopsis thaliana*), although most of the carotenoids are associated with light-harvesting complexes, around 15% of the carotenoids are still freely distributed throughout the thylakoid membrane (Dall'Osto et al. 2010; Zakar et al. 2016), and the lutein/carotene ratio significantly affects thylakoid membrane fluidity (Bykowski et al. 2021).

Does the absence of alka(e)nes affect photosynthesis resilience directly or indirectly?

The measuring and interpretation of chlorophyll fluorescence in cyanobacteria is not as straightforward as in green algae and plants due to the existence of phycobilisomes (Schuurmans et al. 2015). Therefore, in addition to chlorophyll fluorescence measurements, we concurrently performed oxygen evolution measurements on the same sample using MIMS. This dual-measurement approach was adopted specifically to provide a more comprehensive assessment of the photosynthetic capacity of all strains. The Fv/Fm, ΦPSII, and ΦNPQ values we report here do not represent the absolute value of these parameters. However, when interpreted as relative measurements, these results still provide meaningful insights into the photosynthetic performance of all strains. Moreover, we clearly show that oxygen evolution data obtained from our MIMS measurements corroborate the trends observed in the chlorophyll fluorescence data, reinforcing our conclusion of photosynthetic capacity in all strains.

We observed reduced photosynthetic properties when alka(e)ne-deficient strains were exposed to high light. The question is therefore whether the higher sensitivity of photosynthesis to high light in the mutant is caused by the absence of alka(e)nes (due for example to some interaction of alkanes with photosynthetic protein complexes), or if it is caused by the altered membrane lipid composition resulting from alkane(e) deficiency. We believe the latter hypothesis is more likely to be the main cause

Downloaded from https://academic.oup.com/plphys/article/196/1/397/7689884 by The Uppsala Programme for Holocaust and Genocide studies user on 05 November 2024

of the problems in photosynthesis in the mutant but it should be noted that the two hypotheses are not mutually exclusive.

First, previous studies in cyanobacteria and plants have clearly shown that changes in DGDG content affect photosynthesis functionality (Härtel et al. 1997; Sakurai et al. 2007). *Synechocystis* cells lacking DGDG experience stunted growth under high-light conditions, potentially impacting dynamic processes in photosynthesis such as the PSII repair process (Mizusawa et al. 2009). Furthermore, the increased high light sensitivity of alka(e)ene deficient strains may also partly result from changes in the carotenoid composition. It has been shown that carotenoid content, specifically echinenone, increased sharply under high light illumination in both algae and cyanobacteria (Izuhara et al. 2020; Pajot et al. 2023). The sharp increase of echinenone observed in *Synechocystis* WT in response to high light was strongly diminished in the alka(e)ne-deficient strains (Fig. 3E), which could lead to a higher light sensitivity of PSII. Indeed, it has been reported that cells lacking zeaxanthin, echinenone, and myxoxanthophyll show a significant decrease in the capacity for repair of PSII under strong light (Izuhara et al. 2020).

Second, the decrease in the amount of PSI trimers observed in alka(e)ne-deficient strains very likely results from changes in the lipid and carotenoid contents. Indeed, it has been shown in *Arabidopsis thaliana* that DGDG deficiency resulted in a restructuring of the thylakoid domain, causing significant changes in the PSI structure (Ivanov et al. 2006). This structural shift hinders intersystem electron transport and disrupts the regulation of energy distribution via state transitions. The importance of carotenoids in photosynthetic organisms was further revealed with recent findings highlighting their crucial role in the assembly of photosynthetic complexes (Tóth et al. 2015). For instance, xanthophylls, such as echinenone and zeaxanthin, have been pinpointed as instrumental in the fine-tuning of PSI trimerization (Vajravel et al. 2017). This is further illuminated by the crystal structure of the pigment–protein PSI trimeric complex resolved to 2.5 Å using X-ray crystallography (Malavath et al. 2018). Here, echinenone is predominantly situated at the interface between two monomers, with zeaxanthin positioned on the exterior of each monomer, and a single zeaxanthin per monomer. This configuration provides insight into our observations: strains with diminished xanthophyll content exhibit fewer PSI trimers, which is in line with a previous study where the *Synechocystis* mutant lacking xanthophylls showed fewer PSI trimers (Zakar et al. 2017).

Third, a previous study has shown the absence of alka(e)nes results in minor effects on the photosynthetic performance of *Synechocystis* cells (Lea-Smith et al. 2016). In this work, the authors used an intermediate light intensity (40 μmol photons m^{-2} s^{-1}) as compared to our own conditions (10 and 70 μmol photons m^{-2} s^{-1} for low light and high light, respectively). Moreover, the authors did supplement the culture medium with bicarbonate (Lea-Smith et al. 2016), whereas no additional carbon was supplied in our experiments. It seems likely that both light and carbon supply affect the high light phenotype of alka(e)ne-deficient strains; indeed, we observed that when grown in air supplemented with 1% CO_2, the photosynthetic capacity of alka(e)ne-deficient strains is not affected even under high light (70 μmol photons m^{-2} s^{-1}) condition (Supplementary Fig. S11).

Based on the observed phenotypes, we propose therefore the following scenario as the main explanation of photosynthetic deficiency in the mutants (Fig. 4): the absence of alka(e)nes would induce a change in membrane physical properties, such as fluidity, which would trigger compensatory mechanisms including a decrease in DGDG and an increase in MGDG and a change in the carotenoid content. This would in turn induce an instability of PSI trimers and a disturbance of the PSII repair, thus affecting the functioning of the electron transport chain and compromising growth under high light.

In conclusion, our work shows that despite their low abundance, alka(e)nes play a very important role in the lipid composition of cyanobacterial membranes because the absence of these compounds triggers a profound remodeling of the glycerolipid and carotenoid composition. This work also suggests that alka(e)nes have a major role in maintaining basic physicochemical properties of photosynthetic membranes rather than playing a specific role in photosynthesis. This sheds light on the widespread presence of genes encoding alka(e)ne-synthesizing enzymes in the genomes of cyanobacteria and microalgae, organisms of major ecological importance in the global capture of CO_2 by aquatic ecosystems.

Materials and methods

Strains and cultivation conditions

Escherichia coli strains DH5α and XL1-Blue were used for plasmid construction. The cells were grown at 37 °C in LB medium supplemented with corresponding antibiotics for selection. Glucose-tolerant *Synechocystis* PCC6803 was used as background strain in this study, and BG11 medium used here was always buffered to pH = 7.8 by 20 mM TES. To generate knockout mutants, the target gene/operon was replaced with an antibiotic resistance gene through homologous recombination. This was facilitated by two homologous overhangs at both the 5′ and 3′ ends of the target operon or gene, with each overhang being 1000 bp in length. To express FAP in the *slr1993* loci, the *slr1993* gene was replaced by FAP and a spectinomycin resistance gene using homologous recombination. Genetic modifications of all engineered *Synechocystis* strains are explained in Supplementary Table S1, all the primers used in the study are listed in Supplementary Table S2, and all plasmid constructs are shown in Supplementary File S1. Natural transformation was performed using mid-log phase *Synechocystis* culture. For each engineered strain, 3 independent biological replicates were used. Culture maintenance was done using BG11 liquid media or agar plates with corresponding antibiotics. In order to remove the stresses from different antibiotics, the BG11 medium without any antibiotics was used to perform all the experimental culturing. Genotype stability from cultures without antibiotics were confirmed from time to time. Liquid culture cultivation was done in E-flasks with a light source from fluorescent lamp Fluora Osram, and three different light intensities were used: 10 μmol photons m^{-2} s^{-1}, 30 μmol photons m^{-2} s^{-1}, and 70 μmol photons m^{-2} s^{-1}. Cell growth test on BG11-agar plates was performed under three light intensities: 20 μmol photons m^{-2} s^{-1}, 50 μmol photons m^{-2} s^{-1}, and 200 μmol photons m^{-2} s^{-1}. Cell size, number, and volume were measured at each sampling time using a Multisizer Beckman Coulter.

Two previous studies on alkane/alkene-deficient cyanobacterial strains reported difficulties in obtaining fully segregated knockout mutants and a loss of phenotype in glycerol stocks, as well as in cells after several generations on agar plates and in liquid medium (Berla et al. 2015; Lea-Smith et al. 2016). In contrast, our study did not encounter these issues. In our case, we successfully achieved fully segregated mutants after 3 times re-inoculating cells in a fresh BG11 medium containing appropriate antibiotics. The genotype maintained high stability throughout the years of our study. This difference may be due to the low-light conditions used during

Downloaded from https://academic.oup.com/plphys/article/196/1/397/7689884 by The Uppsala Programme for Holocaust and Genocide studies user on 05 November 2024

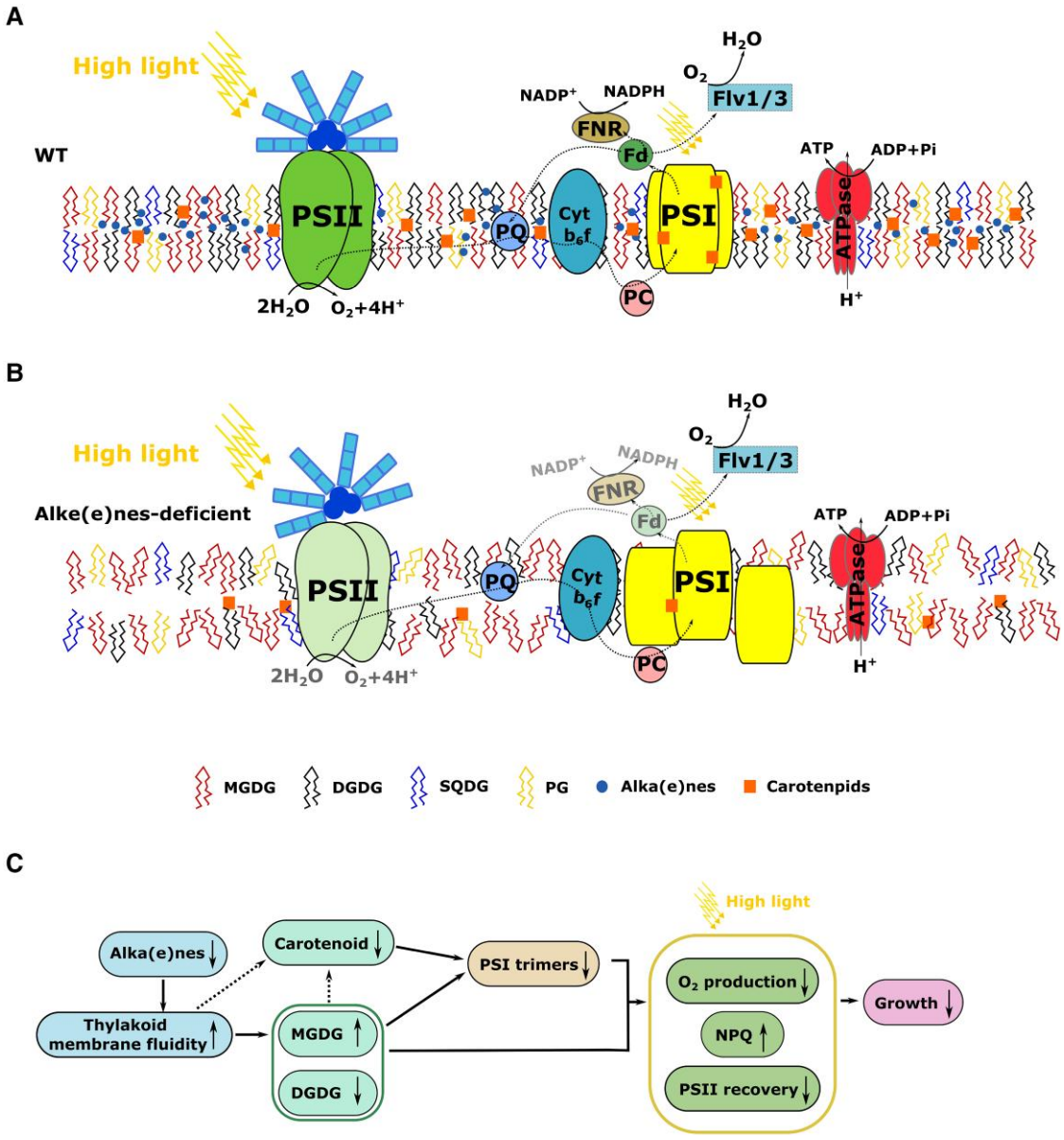

Figure 4. Scheme of the proposed scenario due to alka(e)nes deficiency. **A)** Thylakoid membrane arrangement in wild-type *Synechocystis* cells. **B)** Thylakoid membrane arrangement in alka(e)ne-deficient *Synechocystis* cells. PQ: Plastoquinone, Cytb6f: Cytochrome b6f complex, FNR: Ferredoxin–NADP (+) reductase, Fd: Ferredoxins, PC: plastocyanin, Flv1/3: Flavodiiron proteins Flv1 and Flv3. **C**) Proposed chain of effects resulting from alka(e)nes deficiency. Color coding indicates the different steps of the chain effects.

the selection on agar plates and during culture passage. It is plausible that under low-light conditions, *Synechocystis* may reduce its genome copy number as part of a broader resource conservation strategy to adapt to reduced energy availability. Additionally, we did not observe any loss of phenotype in our cryopreserved stocks prepared using dimethyl sulfoxide as a cryoprotectant.

Lipid extractions

An isopropanol/ methyl-tert-butyl ether (MTBE) method was applied to extract lipids for both LC-MS and HPTLC analysis. Briefly, cultures of the same total cell volume were subjected to centrifugation in a glass tube at 3000 g and 4 °C for 4 min, and the supernatant was subsequently discarded. For each sample, 1 mL of pre-heated isopropanol, supplemented with 10 μL of 1% (w:v) BHT and 1 μL formic acid, was added to the glass tube. Resuspension of the cells was achieved through vigorous vortexing and sonication. For the LC-MS samples, an internal standard of 10 μL was incorporated, while the HPTLC samples did not require an internal standard. The glass tubes, sealed with screw caps, were heated at 85 °C for 10 min to ensure lipase inactivation. Once the samples reached room temperature, 3 mL of methyl-tert-butyl ether (MTBE) was added to each tube and they were shaken vigorously for 2 min. A mixture of 1 mL of 0.9% (v/v) NaCl and 1 μL formic acid was subsequently added to each sample, followed by vigorous shaking. Phase separation was achieved by centrifuging the samples at 3500 g and 4 °C for 2 min. The upper phase was carefully transferred to a new glass tube. A second extraction was initiated by adding 1 mL of MTBE to the remaining lower phase. The upper phases from these two procedures were combined, and the solvent was allowed to evaporate under a stream of nitrogen gas. For LC-MS analysis, lipids were

Downloaded from https://academic.oup.com/plphys/article/196/1/397/7689884 by The Uppsala Programme for Holocaust and Genocide studies user on 05 November 2024

redissolved in 500 μL of a solvent mixture of acetonitrile/isopropanol/ammonium formate (65:30:5, v/v/v). For HPTLC, lipids were resuspended in 400 μL of a freshly prepared chloroform:methanol mixture 2:1 (v:v).

Alka(e)nes and fatty acid analysis

To determine the content of alka(e)nes and fatty acids, 4 mL of each Synechocystis culture in mid-log phase was sampled. It was then centrifuged in a glass tube at 3000 rpm for 10 min. Following this, direct transmethylation was carried out on the harvested cell pellet. Into this pellet, 1 mL of 5% (v/v) H_2SO_4 in methanol, 10 μg of internal standards (*n*-hexadecane and *n*-heptadecanoic acid), and 10 μL of 10% (w/v) butylated hydroxytoluene (BHT) in methanol were added. The resulting mixture in the glass tube was homogenized through sonication. The sealed tube was then heated at 85 °C for 1.5 h. Once it had cooled to room temperature, 1.5 mL of 0.9% (w/v) NaCl was introduced to assist in biphasic separation. Additionally, 500 μL of hexane was added to extract the fatty acid methyl esters and the alka(e)nes. A subsequent centrifugation at 4000 rpm for 4 min was performed, and the hexane layer was collected for further analysis. The hexane extract was injected in an Agilent 7890A gas chromatograph coupled to a Flame Ionization Detector (FID) and an Agilent 5975C mass spectrometer. The column was a Zebron 7HG-G007-11 (Phenomenex) polar capillary column (30 m length, internal diameter of 0.25 mm, film thickness of 0.25 mm). Helium was the carrier gas, with a flow rate maintained at 1 mL min^{-1}. Oven temperature was programmed with an initial 2-min hold time at 60 °C, a first ramp from 60 °C to 150 °C at 15 °C min^{-1}, followed by a 1-min hold time at 170 °C then a second ramp from 170 °C

to 240 °C at 5 °C min^{-1} and a final 2-min hold time at 240 °C. The MS was run in full scan over 40 to 350 amu (electron impact ionization at 70 eV), and peaks of FAMEs and HCs were quantified based on the FID signal using the internal standards C17:0 FAME and hexadecane, respectively. Statistical analyses were done using Prism version 10.2.2(341).

Analysis of lipid classes by HPTLC

Quantification of polar lipids content on HPTLC was carried out as follows: Lipid extracts and polar lipids standards at varying concentrations were applied onto silica gel 60 F254 HPTLC plates (Merck KGaA, Germany) using an ATS 5 automatic TLC sampler (Camag, Switzerland). Subsequently, these plates were developed in an ADC2 automatic developing chamber (Camag) with a solvent mixture of acetone:toluene:water in a ratio of 19:30:8 (v:v:v). Once developed, the plate was allowed to dry thoroughly under a hood. It was then dipped in a CuSO4 reagent for 6 s. After this treatment, the plate was subjected to heating at 141 °C for 30 min. Scanning of the plate was performed using a TLC Scanner 3 operated with WinCATs software (Camag). Lipid classes were quantified based on a standard range for each class.

Lipidomics analysis by LC-MS

Lipid molecular species were analyzed on an ultimate RS 3000 UPLC system (Thermo Fisher, Waltham, MA, USA) connected to a quadrupole-time-of-flight (QTOF) 5600 mass spectrometer (AB Sciex, Framingham, MA, USA) equipped with an ion source operating in negative mode. Lipid extracts were first separated on a Kinetex (Kinetex, Atlanta, GA, USA) C18 2.1 × 150 mm 1.7 μm column (Phenomenex, Torrance, CA, USA). Two solvent mixtures, acetonitrile–water (60:40, v/v) and isopropanol–acetonitrile (90:10, v/v), both containing 10 mM ammonium formate at pH 3.8, were used as eluent A and B respectively. The elution was performed with a gradient of 32 min; eluant B was increased from 27% to 97% in 20 min then maintained for 5 min, solvent B was decreased to 27%, and then maintained for another 7 min for column re-equilibration. The flow rate was 0.3 mL.min-1 and the column oven temperature was maintained at 45 °C. Lipid identification was based on retention time and mass accuracy peaks from the MS survey scan compared with theoretical masses and fragment ions from MS/MS scan. For each molecular species, relative quantification was achieved with Multiquant software (AB Sciex) on the basis of the intensity of the molecular ion of one adduct. Statistical analyses were done using Prism version 10.2.2(341).

Chlorophyll *a*, and carotenoid measurements

The overall concentration determination of chlorophyll a and carotenoid was conducted on the 90% methanol extracts obtained from 1 mL of each *Synechocystis* culture. Absorbance for chlorophyll concentration was taken at 665 nm, while for carotenoid concentration, it was taken at 470 nm. Additionally, absorbance at 720 nm was measured to account for background. The calculations were based on the following equations: Chla[μg/ml] = 12.94*(A665-A720) and Carotenoids[μg/ml] = [1000*(A470-A720)-2.86*(Chla/221)]. For the analysis of molecular species of chlorophylls and carotenoids, pigment extracts were performed on four milliliters of each *Synechocystis* culture by adding 1 mL of pre-cold acetone: methanol 7:2 (v:v) (astaxanthin as internal standard). The mixture was vertex and sonicated for 5 min, stored in −20 °C for 1.5 h, and followed by 10 min centrifugation at 4 °C. Identification and quantification of pigments were performed by LC-MS using commercial standards as well as the same conditions as for glycerolipid analysis except that ionization was in positive mode. Statistical analyses were done using Prism version 10.2.2(341).

Chlorophyll fluorescence and oxygen evolution measurements

Chlorophyll fluorescence and oxygen evolution were simultaneously measured using pulsed amplitude modulation (PAM) fluorimeter (Dual-PAM 100) coupled with the MIMS setup (Burlacot et al. 2020). Two milliliters of cell suspension at a final chlorophyll content of 5 μg Chl ml^{-1} was placed in a flat bottom stirred temperature-controlled (30 °C) cuvette placed in darkness for 10, and 10 μL of 0.5 M $NaHCO_3$ was added. The cell suspension was bubbled with ^{18}O-enriched O_2 (with 99% $^{18}O_2$ isotope content from Euriso-Top) until concentrations of $^{16}O_2$ and $^{18}O_2$ reached approximately equal values. Both oxygen exchange and chlorophyll fluorescence were then measured in the dark for 3 min and then in response to stepwise increase of blue actinic light intensity up to 6200 μmol photons m^{-2} s^{-1}. The use of 460 nm blue actinic light was to mitigate the influence of phycobilisomes on chlorophyll fluorescence measurement in cyanobacteria. NPQ was determined as (Fm-Fm")/Fm" based on the chlorophyll fluorescence Fm measured in darkness. Meanwhile, O_2 uptake, gross O_2 production and net O_2 evolution rates were measured on the same sample using MIMS as described in a previous study (Burlacot et al. 2020). Statistical analyses were done using Prism version 10.2.2(341).

Downloaded from https://academic.oup.com/plphys/article/196/1/397/7689884 by The Uppsala Programme for Holocaust and Genocide studies user on 05 November 2024

Thylakoid extraction and native PAGE

Cells with an OD_{730} ranging from 0.5 to 0.8, were harvested from a fifty-milliliter sample via centrifugation at 2300 g and 4 °C for 10 min. The resultant pellet was then resuspended in 150 μL of thylakoid buffer (containing 25 mM MES-NaOH at pH 6.5, 10 mM $CaCl_2$, 10 mM $MgCl_2$, and 25% (w/v) glycerol) and relocated to a 2-mL screw cap tube. A set of glass beads from a PCR tube was introduced to the tube, followed by cell disruption using a liquid nitrogen-paired BeadBeater. Subsequently, 200 μL of the thylakoid buffer was added, the mixture was vortexed twice, and the supernatant was transferred to a new, chilled Eppendorf tube. This procedure was repeated five times. To separate any remaining unbroken cells and glass beads, the mixture was centrifuged at 4000 g for a minute. The clear supernatant was then moved to another cooled Eppendorf tube and subjected to further centrifugation at 16,000 g and 4 °C for 20 min. After discarding the supernatant, the pellet was resuspended in 200 μL of thylakoid buffer with the aid of a stainless-steel piston and vortexing. For membrane solubilization, a tenth of the volume of freshly prepared 10% (v/v) *n*-Dodecyl-β-D-maltoside (DM) was added to the samples, which were then incubated on ice for 5 min. Chlorophyll extraction from the samples was performed using methanol, and its concentration was determined spectrophotometrically. Afterward, the solubilized membrane sample, containing 10 μg of chlorophyll, was centrifuged again under the same conditions. The resultant supernatant was transferred to a new chilled Eppendorf tube and mixed with 10% (v/v) deoxycholate (DOC) to achieve a final DOC concentration of 0.5%. This mixture was then loaded onto a Mini-PROTEAN TGX Gel (BioRad) for clear-native PAGE. The buffer system used for the native PAGE consisted of an upper buffer (with 0.05 M tricine, 15 mM Bis–Tris/HCl at pH 7, 0.05% (v/v) DOC, and 0.02% (v/v) DM) and a lower buffer (0.05 M Bis–Tris/HCl at pH 7). Importantly, all extraction and native PAGE procedures were conducted at 4 °C and shielded from light.

Transmission electron microscopy

Synechocystis cells in the mid-log phase (OD_{730} = 0.5 to 0.8) were subjected to centrifugation at 3000 g and 4 °C for 10 min. Subsequently, the cells were fixed in 2.5% (v/v) glutaraldehyde combined with 1% (v/v) paraformaldehyde and 0.1 M PIPES. This fixation process was carried out for 60 min on a shaker at room temperature. For embedding, the cells underwent a series of treatments: (1) Rinsing in 0.1 M PB for 10 min; (2) a 120-min incubation in 0.1 M PB containing 1% (v/v) Osmium tetroxide was applied; (3) another 10-min rinse in 0.1 M PB followed; (4) the cells were sequentially exposed to increasing concentrations of ethanol (ranging from 50% to 100% (v/v), with each concentration applied for 10 min; (5) a 30-minute incubation in a 100% ethanol:LR white resin mixture in a 1:1 (v/v) ratio was done; (6) an overnight immersion in LR white resin took place, after which the medium was replaced with fresh LR white acrylic resins; and (7) curing at 60 °C for 48 h. Between each of the aforementioned steps, the cells were settled by centrifuging at 2300 g for 2 min. Ultra-thin sections, between 70 and 80 nm in thickness, were sliced using a Leica UCT Ultramicrotome and carefully positioned on grids. These grids were then treated with stains: 2% (v/v) uranyl acetate followed by 3% (v/v) Reynolds lead citrate. Finally, the stained specimens were analyzed using a TEM (FEI Tecnai G2) operating at 80 kV. The mean of thylakoid membrane layer numbers of 20 individual cells for each strain was calculated, and one-way ANOVA was used to determine statistical significance. Statistical analyses were done using Prism version 10.2.2(341).

Accession numbers

Sequence data from this article can be found in the data libraries under accession numbers: *sll0208* GenBank: BAA10217.1; *sll0209* GenBank: BAA10216.1; *slr1993* GenBank: BAA17882.1; FAP PDB: 5NCC_A.

Acknowledgments

We acknowledge the excellent internship work of Ms. Emma Calikanzaros who contributed to part of this study. We also acknowledge the BioVis facility at Uppsala University for providing the service on transmission electron microscopy.

Author contributions

R.M. designed and coordinated the study, performed experiments including cloning of strains, cultivation, alkanes, fatty acids and lipids extraction, pigments and thylakoid extractions, lipid quantification using HPTLC, native PAGE, chlorophyll fluorescence measurement, oxygen evolution measurement, and sample preparation for electron microscopy, and wrote the manuscript; B.L. performed all measurements on HPLC-MS, and lipidomics data analysis; S.C. performed alkanes and fatty acids measurements on GC-MS, and supervised on native PAGE and daily lab practices; A.B. supervised on growth test and chlorophyll fluorescence measurement, and provided helpful discussions; P.L. provided experimental facilities for transmission electron microscopy sample preparation; Y.L-B. provided helpful discussions and suggestions to the project, and wrote the manuscript; F.B. supervised the project and provided helpful discussions and suggestions to the project, and wrote the manuscript; G.P. supervised and coordinated the project and performed oxygen evolution measurements, and wrote the manuscript.

Supplementary data

The following materials are available in the online version of this article.

Supplementary Figure S1. Growth under different light intensities and alka(e)ne content of each strain.

Supplementary Figure S2. Transmission electron microscopy images.

Supplementary Figure S3. Quantity of thylakoid layers per cell.

Supplementary Figure S4. Original Clear-Native PAGE photos on thylakoid membrane extracts.

Supplementary Figure S5. Membrane inlet mass spectrometry (MIMS) measured O_2 uptake and net O_2 evolution rates from cells grown under low-light and high light intensities.

Supplementary Figure S6. Scheme of central metabolic pathways relate to alka(e)nes synthesis in *Synechocystis* PCC 6803

Supplementary Figure S7. Proportion of saturated-, unsaturated-, and cyclo-fatty acid under low and high light.

Supplementary Figure S8. Polar lipid quantification using high-performance thin-layer chromatography (HPTLC).

Supplementary Figure S9. Chlorophyll content measured on liquid chromatography-mass spectrometry (LC-MS).

Supplementary Figure S10. Spectrophotometer measured carotenoids to chlorophyll content ratio in cells cultivated under 70 μmol photons m^{-2} s^{-1} light with 1% CO_2.

Supplementary Figure S11. Chlorophyll fluorescence measured on cells grown at atmospheric level or 1% CO_2 conditions.

Supplementary Table S1. List of engineered strains and genetic constructs.

Downloaded from https://academic.oup.com/plphys/article/196/1/397/7689884 by The Uppsala Programme for Holocaust and Genocide studies user on 05 November 2024

Supplementary Table S2. All primers used in the study.
Supplementary File 1. Plasmid constructs.

Funding

This work was funded by the French National Research Agency (ANR) project Photoalkane (ANR-18-CE43-0008). We thank the Torsten Thuréns stiftelse för miljövänlig forskning for providing financial support for the transmission electron microscopy experiment. The Federation of European Microbiological Societies (FEMS) provided a research training grant for completing part of the photosynthetic capacity measurements. The European Union Regional Developing Fund (ERDF), the Région Provence Alpes Côte d'Azur, the French Ministry of Research, and the CEA for funding the HelioBiotec platform.

Conflict of interest statement. The authors declare that there is no potential conflict of interest.

Data availability

The data underlying this article will be shared on reasonable request to the corresponding author.

References

Berla BM, Saha R, Maranas CD, Pakrasi HB. Cyanobacterial alkanes modulate photosynthetic cyclic electron flow to assist growth under cold stress. *Sci Rep.* 2015:5(1):14894. https://doi.org/10.1038/srep14894

Blomquist GJ, Ginzel MD. Chemical ecology, biochemistry, and molecular biology of insect hydrocarbons. *Annu Rev Entomol.* 2021:66(1):45–60. https://doi.org/10.1146/annurev-ento-031620-071754

Burlacot A, Burlacot F, Li-Beisson Y, Peltier G. Membrane inlet mass spectrometry: a powerful tool for algal research. *Front Plant Sci.* 2020:11:1302. https://doi.org/10.3389/fpls.2020.01302

Bykowski M, Mazur R, Wójtowicz J, Suski S, Garstka M, Mostowska A, Kowalewska Ł. Too rigid to fold: carotenoid-dependent decrease in thylakoid fluidity hampers the formation of chloroplast grana. *Plant Physiol.* 2021:185(1):210–227. https://doi.org/10.1093/plphys/kiaa009

Chung H, Carroll SB. Wax, sex and the origin of species: dual roles of insect cuticular hydrocarbons in adaptation and mating. *BioEssays.* 2015:37(7):822–830. https://doi.org/10.1002/bies.201500014

Coates RC, Podell S, Korobeynikov A, Lapidus A, Pevzner P, Sherman DH, Allen EE, Gerwick L, Gerwick WH. Characterization of cyanobacterial hydrocarbon composition and distribution of biosynthetic pathways. *PloS one.* 2014:9(1):e85140. https://doi.org/10.1371/journal.pone.0085140

Dall'Osto L, Cazzaniga S, Havaux M, Bassi R. Enhanced photoprotection by protein-bound vs free xanthophyll pools: a comparative analysis of chlorophyll b and xanthophyll biosynthesis mutants. *Mol Plant.* 2010:3(3):576–593. https://doi.org/10.1093/mp/ssp117

Dhami N, Drake JE, Tjoelker MG, Tissue DT, Cazzonelli CI. An extreme heatwave enhanced the xanthophyll de-epoxidation state in leaves of Eucalyptus trees grown in the field. *Physiol Mol Biol Plants Int J Funct Plant Biol.* 2020:26(2):211–218. https://doi.org/10.1007/s12298-019-00729-6

Härtel H, Dormann P, Benning C. DGD1-independent biosynthesis of extraplastidic galactolipids after phosphate deprivation in *Arabidopsis*. *Proc Natl Acad Sci USA.* 2000:97(19):10649–10654. https://doi.org/10.1073/pnas.180320497

Härtel H, Lokstein H, Dormann P, Grimm B, Benning C. Changes in the composition of the photosynthetic apparatus in the galactolipid-deficient dgd1 mutant of Arabidopsis thaliana. *Plant Physiol.* 1997:115(3):1175–1184. https://doi.org/10.1104/pp.115.3.1175

Havaux M. Carotenoids as membrane stabilizers in chloroplasts. *Trends Plant Sci.* 1998:3(4):147–151. https://doi.org/10.1016/S1360-1385(98)01200-X

Herman NA, Zhang W. Enzymes for fatty acid-based hydrocarbon biosynthesis. *Curr Opin Chem Biol.* 2016:35:22–28. https://doi.org/10.1016/j.cbpa.2016.08.009

Hoyo J, Guaus E, Torrent-Burgués J. Monogalactosyldiacylglycerol and digalactosyldiacylglycerol role, physical states, applications and biomimetic monolayer films. *Eur Phys J E Soft Matter.* 2016:39(3):39. https://doi.org/10.1140/epje/i2016-16039-0

Ivanov AG, Hendrickson L, Krol M, Selstam E, Öquist G, Hurry V, Huner NPA. Digalactosyl-diacylglycerol deficiency impairs the capacity for photosynthetic intersystem electron transport and state transitions in Arabidopsis thaliana due to photosystem I acceptor-side limitations. *Plant Cell Physiol.* 2006:47(8):1146–1157. https://doi.org/10.1093/pcp/pcj089

Izuhara T, Kaihatsu I, Jimbo H, Takaichi S, Nishiyama Y. Elevated levels of specific carotenoids during acclimation to strong light protect the repair of photosystem II in synechocystis sp. PCC 6803. *Front Plant Sci.* 2020:11:1030. https://doi.org/10.3389/fpls.2020.01030

Kirilovsky D, Kerfeld CA. The orange carotenoid protein in photoprotection of photosystem II in cyanobacteria. *Biochim Biophys Acta.* 2012:1817(1):158–166. https://doi.org/10.1016/j.bbabio.2011.04.013

Klähn S, Baumgartner D, Pfreundt U, Voigt K, Schon V, Steglich C, Hess WR. Alkane biosynthesis genes in Cyanobacteria and their transcriptional organization. *Front Bioeng Biotechnol.* 2014:2:24. https://doi.org/10.3389/fbioe.2014.00024

Koch M, Berendzen KW, Forchhammer K. On the role and production of polyhydroxybutyrate (PHB) in the cyanobacterium synechocystis sp. PCC 6803. *Life (Basel, Switzerland).* 2020:10(4):47. https://doi.org/10.3390/life10040047

Laurent P, Braekman J-C, Daloze D, Pasteels J. Biosynthesis of defensive compounds from beetles and ants. *European J Org Chem.* 2003:2003(15):2733–2743. https://doi.org/10.1002/ejoc.200300008

Lea-Smith DJ, Biller SJ, Davey MP, Cotton CAR, Perez Sepulveda BM, Turchyn AV, Scanlan DJ, Smith AG, Chisholm SW, Howe CJ. Contribution of cyanobacterial alkane production to the ocean hydrocarbon cycle. *Proc Natl Acad Sci USA.* 2015:112(44):13591–13596. https://doi.org/10.1073/pnas.1507274112

Lea-Smith DJ, Ortiz-Suarez ML, Lenn T, Nürnberg DJ, Baers LL, Davey MP, Parolini L, Huber RG, Cotton CAR, Mastroianni G, *et al.* Hydrocarbons are essential for optimal cell size, division, and growth of Cyanobacteria. *Plant Physiol.* 2016:172(3):1928–1940. https://doi.org/10.1104/pp.16.01205

Lee SB, Suh MC. Regulatory mechanisms underlying cuticular wax biosynthesis. *J Exp Bot.* 2022:73(9):2799–2816. https://doi.org/10.1093/jxb/erab509

Li N, Nørgaard H, Warui DM, Booker SJ, Krebs C, Bollinger JM. Conversion of fatty aldehydes to alka(e)nes and formate by a cyanobacterial aldehyde decarbonylase: cryptic redox by an unusual dimetal oxygenase. *J Am Chem Soc.* 2011:133(16):6158–6161. https://doi.org/10.1021/ja2013517

Love CR, Arrington EC, Gosselin KM, Reddy CM, Van Mooy BAS, Nelson RK, Valentine DL. Microbial production and consumption of hydrocarbons in the global ocean. *Nat Microbiol.* 2021:6(4):489–498. https://doi.org/10.1038/s41564-020-00859-8

Downloaded from https://academic.oup.com/plphys/article/196/1/397/7689884 by The Uppsala Programme for Holocaust and Genocide studies user on 05 November 2024

Major MA, Blomquist GJ. Biosynthesis of hydrocarbons in insects: decarboxylation of long chain acids ton-alkanes inPeriplaneta. *Lipids*. 1978:13(5):323–328. https://doi.org/10.1007/bf02533722

Malavath T, Caspy I, Netzer-El SY, Klaiman D, Nelson N. Structure and function of wild-type and subunit-depleted photosystem I in synechocystis. *Biochim Biophys Acta Bioenergetics*. 2018:1859(9)(9):645–654. https://doi.org/10.1016/j.bbabio.2018.02.002

Marsh D. Components of the lateral pressure in lipid bilayers deduced from HII phase dimensions. *Biochim Biophys Acta*. 1996:1279(2): 119–123. https://doi.org/10.1016/0005-2736(95)00296-0

Mendez-Perez D, Begemann MB, Pfleger BF. Modular synthase-encoding gene involved in α-olefin biosynthesis in synechococcus sp. Strain PCC 7002. *Appl Environ Microbiol*. 2011:77(12):4264–4267. https://doi.org/10.1128/AEM.00467-11

Mizusawa N, Sakurai I, Sato N, Wada H. Lack of digalactosyldiacylglycerol increases the sensitivity of synechocystis sp. PCC 6803 to high light stress. *FEBS Lett*. 2009:583(4):718–722. https://doi.org/10.1016/j.febslet.2009.01.021

Moulin SLY, Beyly-Adriano A, Cuiné S, Blangy S, Légeret B, Floriani M, Burlacot A, Sorigué D, Samire P-P, Li-Beisson Y, *et al*. Fatty acid photodecarboxylase is an ancient photoenzyme that forms hydrocarbons in the thylakoids of algae. *Plant Physiol*. 2021:186(3): 1455–1472. https://doi.org/10.1093/plphys/kiab168

Pagels F, Vasconcelos V, Guedes AC. Carotenoids from Cyanobacteria: biotechnological potential and optimization strategies. *Biomolecules*. 2021:11(5):735. https://doi.org/10.3390/biom11050735

Pajot A, Lavaud J, Carrier G, Lacour T, Marchal L, Nicolau E. Light-response in two clonal strains of the haptophyte tisochrysis lutea: evidence for different photoprotection strategies. *Algal Res*. 2023:69:102915. https://doi.org/10.1016/j.algal.2022.102915

Sakurai I, Mizusawa N, Wada H, Sato N. Digalactosyldiacylglycerol is required for stabilization of the oxygen-evolving complex in photosystem II. *Plant Physiol*. 2007:145(4):1361–1370. https://doi.org/10.1104/pp.107.106781

Samire PP, Zhuang B, Légeret B, Baca-Porcel A, Peltier G, Sorigué D, Aleksandrov A, Beisson F, Müller P. Autocatalytic effect boosts the production of medium-chain hydrocarbons by fatty acid photodecarboxylase. *Sci Adv*. 2023:9(13):eadg3881. https://doi.org/10.1126/sciadv.adg3881

Schirmer A, Rude MA, Li X, Popova E, del Cardayre SB. Microbial biosynthesis of alkanes. *Science*. 2010:329(5991):559–562. https://doi.org/10.1126/science.1187936

Schuurmans RM, van Alphen P, Schuurmans JM, Matthijs HCP, Hellingwerf KJ. Comparison of the photosynthetic yield of Cyanobacteria and green algae: different methods give different answers. *PLoS One*. 2015:10(9):e0139061. https://doi.org/10.1371/journal.pone.0139061

Sorigué D, Hadjidemetriou K, Blangy S, Gotthard G, Bonvalet A, Coquelle N, Samire P, Aleksandrov A, Antonucci L, Benachir A, *et al*. Mechanism and dynamics of fatty acid photodecarboxylase. *Science*. 2021:372(6538):eabd5687. https://doi.org/10.1126/science.abd5687

Sorigué D, Légeret B, Cuiné S, Blangy S, Moulin S, Billon E, Richaud P, Brugière S, Couté Y, Nurizzo D, *et al*. An algal photoenzyme converts fatty acids to hydrocarbons. *Science*. 2017:357(6354):903–907. https://doi.org/10.1126/science.aan6349

Sorigué D, Légeret B, Cuiné S, Morales P, Mirabella B, Guédeney G, Li-Beisson Y, Jetter R, Peltier G, Beisson F. Microalgae synthesize hydrocarbons from long-chain fatty acids via a light-dependent pathway. *Plant Physiol*. 2016:171(4):2393–2405. https://doi.org/10.1104/pp.16.00462

Tóth TN, Chukhutsina V, Domonkos I, Knoppová J, Komenda J, Kis M, Lénárt Z, Garab G, Kovács L, Gombos Z, *et al*. Carotenoids are essential for the assembly of cyanobacterial photosynthetic complexes. *Biochim Biophys Acta*. 2015:1847(10):1153–1165. https://doi.org/10.1016/j.bbabio.2015.05.020

Vajravel S, Kis M, Kłodawska K, Laczko-Dobos H, Malec P, Kovács L, Gombos Z, Toth TN. Zeaxanthin and echinenone modify the structure of photosystem I trimer in synechocystis sp. PCC 6803. *Biochim Biophys Acta Bioenergetics*. 2017:1858(7):510–518. https://doi.org/10.1016/j.bbabio.2017.05.001

Valderrama B. Chapter 13 bacterial hydrocarbon biosynthesis revisited. In: Vazquez-Duhalt R, Quintero-Ramirez R, editors. *Studies in surface science and catalysis*. Elsevier; 2004. p. 373–384. https://doi.org/10.1016/S0167-2991(04)80154-X

Vuorio E, Thiel K, Fitzpatrick D, Huokko T, Kämäräinen J, Dandapani H, Aro E-M, Kallio P. Hydrocarbon desaturation in cyanobacterial thylakoid membranes is linked with acclimation to suboptimal growth temperatures. *Front Microbiol*. 2021:12. https://doi.org/10.3389/fmicb.2021.781864

Yamamori T, Kageyama H, Tanaka Y, Takabe T. Requirement of alkanes for salt tolerance of Cyanobacteria: characterization of alkane synthesis genes from salt-sensitive synechococcus elongatus PCC7942 and salt-tolerant aphanothece halophytica. *Lett Appl Microbiol*. 2018:67(3):299–305. https://doi.org/10.1111/lam.13038

Yeats TH, Rose JKC. The formation and function of plant cuticles. *Plant Physiol*. 2013:163(1):5–20. https://doi.org/10.1104/pp.113.222737

Zakar T, Herman E, Vajravel S, Kovacs L, Knoppová J, Komenda J, Domonkos I, Kis M, Gombos X, Laczko-Dobos H. Lipid and carotenoid cooperation-driven adaptation to light and temperature stress in Synechocystis sp. PCC6803. *Biochim Biophys Acta Bioenergetics*. 2017:1858(5):337–350. https://doi.org/10.1016/j.bbabio.2017.02.002

Zakar T, Laczko-Dobos H, Toth TN, Gombos Z. Carotenoids assist in cyanobacterial photosystem II assembly and function. *Front Plant Sci*. 2016:7:295. https://doi.org/10.3389/fpls.2016.00295

Downloaded from https://academic.oup.com/plphys/article/196/1/397/7689884 by The Uppsala Programme for Holocaust and Genocide studies user on 05 November 2024